

## Article

# Monitoring Mangrove Forest Degradation and Regeneration: Landsat Time Series Analysis of Moisture and Vegetation Indices at Rabigh Lagoon, Red Sea

Mohammed Othman Aljahdali <sup>1,\*</sup>, Sana Munawar <sup>2</sup> and Waseem Razzaq Khan <sup>3,4,\*</sup>

<sup>1</sup> Department of Biological Sciences, Faculty of Science, King Abdulaziz University (KAU), P.O. Box 80203, Jeddah 21589, Saudi Arabia

<sup>2</sup> Umweltfernerkundung und Geoinformatik, Universität Trier, 54296 Trier, Germany; s6ssmuna@uni-trier.de

<sup>3</sup> Department of Forestry Science and Biodiversity, Faculty of Forestry and Environment, Universiti Putra Malaysia, Sri Serdang, Selangor 43300, Malaysia

<sup>4</sup> Institut Ekosains Borneo, Universiti Putra Malaysia Kampus Bintulu, Sarawak 97008, Malaysia

\* Correspondence: moaljahdali@kau.edu.sa (M.O.A.); khanwaseem@upm.edu.my (W.R.K.)

**Abstract:** Rabigh Lagoon, located on the eastern coast of the Red Sea, is an ecologically rich zone in Saudi Arabia, providing habitat to *Avicennia marina* mangrove trees. The environmental quality of the lagoon has been decaying since the 1990s mainly from sedimentation, road construction, and camel grazing. However, because of remedial measures, the mangrove communities have shown some degree of restoration. This study aims to monitor mangrove health of Rabigh Lagoon during the time it was under stress from road construction and after the road was demolished. For this purpose, time series of EVI (Enhanced Vegetation Index), MSAVI (Modified, Soil-Adjusted Vegetation Index), NDVI (Normalized Difference Vegetation Index), and NDMI (Normalized Difference Moisture Index) have been used as a proxy to plant biomass and indicator of forest disturbance and recovery. Long-term trend patterns, through linear, least square regression, were estimated using 30 m annual Landsat surface-reflectance-derived indices from 1986 to 2019. The outcome of this study showed (1) a positive trend over most of the study region during the evaluation period; (2) most trend slopes were gradual and weakly positive, implying subtle changes as opposed to abrupt changes; (3) all four indices divided the times series into three phases: degraded mangroves, slow recovery, and regenerated mangroves; (4) MSAVI performed best in capturing various trend patterns related to the greenness of vegetation; and (5) NDMI better identified forest disturbance and recovery in terms of water stress. Validating observed patterns using only the regression slope proved to be a challenge. Therefore, water quality parameters such as salinity, pH/dissolved oxygen should also be investigated to explain the calculated trends.

**Keywords:** forest change; degradation; regeneration; geospatial-temporal analysis; trend



**Citation:** Aljahdali, M.O.; Munawar, S.; Khan, W.R. Monitoring Mangrove Forest Degradation and Regeneration: Landsat Time Series Analysis of Moisture and Vegetation Indices at Rabigh Lagoon, Red Sea. *Forests* **2021**, *12*, 52. <https://doi.org/10.3390/f12010052>

Received: 15 October 2020

Accepted: 15 December 2020

Published: 1 January 2021

**Publisher's Note:** MDPI stays neutral with regard to jurisdictional claims in published maps and institutional affiliations.



**Copyright:** © 2021 by the authors. Licensee MDPI, Basel, Switzerland. This article is an open access article distributed under the terms and conditions of the Creative Commons Attribution (CC BY) license (<https://creativecommons.org/licenses/by/4.0/>).

## 1. Introduction

Mangrove swamps are a common feature in coastal areas that are exposed to the daily fluctuation of tides. They are predominantly found in muddy substrate with low wave energy and hypersaline environment [1–7]. Mangroves serve as an important habitat for fish communities and other benthic flora and fauna [8]. Moreover, they play a key role in shoreline protection and waste assimilation through the purification of marine water and surrounding air. Mangroves are also important for carbon sequestration since they are a major sink for carbon by storing it in the sediments [9,10]. In addition, mangrove trees have shown great tolerance to low levels of dissolved oxygen in coastal environments [11–14].

The spatial distribution of mangrove trees along the Red Sea coast of Saudi Arabia was found in 104 locations with an estimated total area of 3452 hectares (ha) [15]. Two major species common to this area are *Avicennia marina* and *Rhizophora mucronata*. Lagoons

share 15% of the globe's coastal areas. Mangrove swamps of Red Sea are essential for various ecological functions such as nursery for commercial fish species [16], protection of coral reefs [17], and provision of nesting sites for bird species like Goliath heron and Reef heron [18]. There has been an observed degradation of mangrove trees in the Red Sea region. Some of the major drivers of degradation are the clearing of large areas of mangrove for hardwood, shrimp farming, over grazing by camels, construction activities that alter the water level, and tidal flow. For instance, building dams has significantly lowered fresh water flow into the swamps, thereby, leading to a substantial rise in the level of salinity [19]. In addition to that, mangrove species of this region grow in a particularly harsh environment including: salinity levels of more than 40 ppt, sea surface temperature of more than 31 °C in summers, and no permanent source of freshwater recharge [20].

In the context of the Rabigh lagoon, in 1987, a new road was constructed in the northwest of the study area crossing the mouth of the bay. This road obstructed the recurrence of water flow within the swamp. As a result, the amount of freshwater flow decreased and salinity of the bay area gradually elevated, thereby reducing the productivity of the mangrove trees. By the end of 2012, the road was flooded by sea water, completely opening the bay, and consequently improving the health of mangroves due to the enhancement of water movement.

In order to conserve ecologically sensitive regions, it is inevitable to first monitor their status. Remotely sensed data, especially multi-spectral Landsat data, have been widely used for such purposes [21–25]. Essentially the spectral information from satellite imagery is used to correlate it with the biophysical properties of vegetation cover. Several studies have indicated that the NDVI (Normalized Difference Vegetation Index) of mangrove represents high correlation with biomass and leaf area index [26–30]. Other indices such as Enhanced Vegetation Index (EVI) and Soil Adjusted Vegetation Index (SAVI) are also used to monitor plant health as they are most robust than NDVI. For instance, EVI is sensitive to background canopy variations and does not saturate over high biomass. SAVI accounts for background soil component that can interfere with the vegetation signal [31]. Normalized Difference Moisture Index (NDMI) has been used to detect forest disturbance and recovery since it detects variation in the moisture content of the vegetation. It can differentiate between the moisture content of soil and vegetation and is less sensitive to atmospheric scattering; SWIR (shortwave infrared) used for NDMI can penetrate thin clouds as well [32].

Alamahasheer et al. [33] studied changes in Red Sea mangroves using multi-temporal Landsat imagery, Elsebaie et al. [34] used integrated remote sensing and GIS (geographic information system) approach to identify suitable plantation sites for mangroves on the southern coast of the Red Sea, Kumar et al. [35] surveyed distribution of mangroves along the coast of the Red Sea using NDVI, and Monsef and Smith [36] estimated mangrove cover in the Red Sea using Landsat spectral indices. This study aims to monitor the status of mangrove trees in Rabigh Lagoon by comparing spatial and temporal patterns during the time of obstructed water circulation and after the water circulation was resumed. To our knowledge, this is the first study to use hyper temporal data and trend estimation, over this region, in the form of annual images for the past 34 years.

## 2. Materials and Methods

### 2.1. Study Area

Rabigh Lagoon is located on the northeast coast of Red Sea. It, also called as Sharm El Kharar, extends between longitudes 38° E and 39° E and latitudes 22° N and 23° N. Its origin dates to late Pleistocene because of erosion, followed by flooding due to postglacial sea level rise in early Holocene transgression [37–39]. The study region is only 16 km from Rabigh city and occupies an area of about 75 km<sup>2</sup> (Figure 1) with many patches of mangrove communities spreading over an area of 136.7 ha [35]. Surface elevation of the area differs widely from –10 to 58.5 m above sea level. Sediment texture is mostly mud, gravelly sand, and sandy mud. The prevailing climate is dry and tropical. In winters, there is also influx of freshwater from wadis: Rabigh, Rehab, Murayykh, and Al-Khariq.

Tidal range is 20 to 30 cm. Water exchange between the lagoon and the sea takes place mainly via the following process: Water, having temperature of 25 to 30 °C and salinity of 39‰, enters the lagoon as surface inflow. After circulating the lagoon, it exits in the form of subsurface flow with relatively similar temperature and a salinity of 39.8‰ and 40.5‰ during winter and summer, respectively [40]. On average, it takes 15 days for the water to circulate the lagoon, with the speed of flow of 50 cm per second at the entrance 5–20 cm per second inside the lagoon. *Avicennia marina* is the only mangrove species that is found in the lagoon [41]. They mostly have a stunted growth reaching to a height of 2 m. The Rabigh lagoon has suffered from climatic changes and global warming in the form of increased water temperature and sea level rise [42].

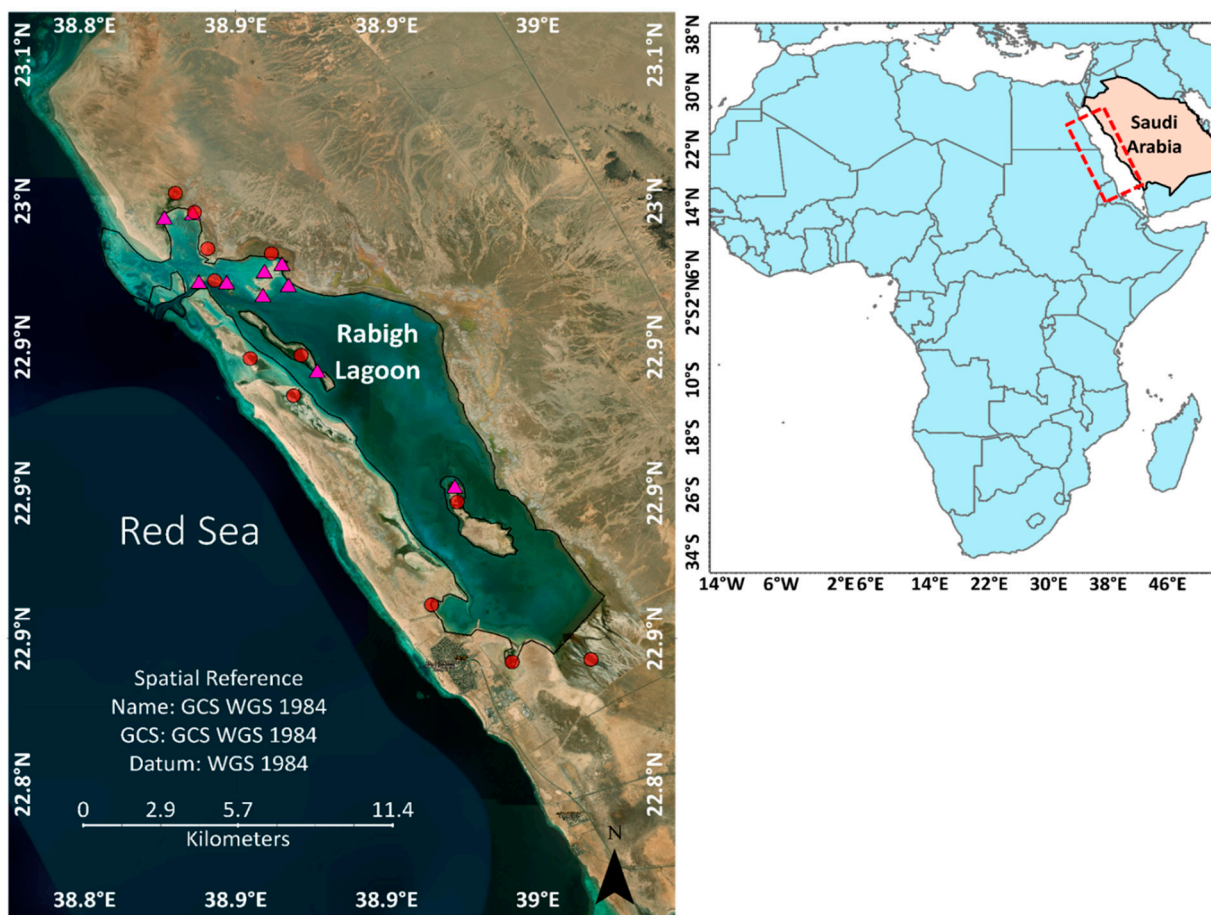


**Figure 1.** Map of study site, Rabigh Lagoon, located along the coast of Red Sea, Saudi Arabia. Pink triangles show locations for field visits. Red dots show locations from where pixel wise time series were extracted. GCS stands for Geographic Coordinate System. WGS stands for World Geodetic System.

## 2.2. Trend Analysis Using Time Series

Time series are data points distributed across equal intervals. Time series of vegetation indices have been used for ecological studies such as monitoring forest and land degradation. This study used 30 m annual images, from 1986 to 2019, generated from sensors onboard Landsat 5 (1986 to 2002), Landsat 7 (2003 to 2012), and Landsat 8 (2013 to 2019) to derive the long-term trend component over mangrove forests in the study region. The different indices used were as follows (Table 1): NDVI, EVI, MSAVI, and NDMI. Images for all years belonged to the summer season, which is June to September, depending on data availability and minimum cloud cover. Data were obtained from the online archive of USGS EROS (United States Geological Survey Earth Resources Observation and Science) Center Science Processing Architecture. The final product (normalized indices) downloaded, with path row 170/044 on WRS-2 (World Reference system), was derived using

surface reflectance (tier 1) products from Landsat 5 TM (Thematic Mapper), Landsat 7 ETM (Enhanced Thematic Mapper), and Landsat 8 OLI (Operational Land Imager). Surface reflectance products are radiometrically and atmospherically corrected and come along with cloud, shadow, water, and snow masks developed using the CFMASK (C Function of Mask) algorithm. More information about Landsat surface reflectance product characteristics can be found in Schmidt et al. [43] and Vermote et al. [44] findings. All images were rescaled to fall in the range between  $-1$  to  $1$  by multiplying the values with  $0.0001$ . Images from Landsat 7 between the years 2003 and 2012 with SLC (Scan Line Corrector) failure were gap filled using linear interpolation. All non-vegetated areas and water bodies were masked out from further analysis using a threshold median EVI of  $0.08$ . This threshold was determined by comparing EVI values of vegetation with non-vegetated surface around Rabigh Lagoon. Figure 2 shows spatial distribution of prominent vegetation communities (dark green tones).

**Table 1.** Spectral indices used for time series analysis.

Spectral Index	Formula	Wavelength ( $\mu\text{m}$ )	Reference	
NDVI	$(\text{NIR} - \text{Red})/(\text{NIR} + \text{Red})$	Red	$0.63\text{--}0.69$	[45]
EVI	$G * (\text{NIR} - \text{Red})/(\text{NIR} + \text{C1} * \text{Red} - \text{C2} * \text{Blue} + \text{L})$	Blue	$0.45\text{--}0.52$	[46]
MSAVI	$(2 * \text{NIR} + 1 - \text{sqrt}((2 * \text{NIR} + 1)^2 - 8 * (\text{NIR} - \text{Red}))/2)$	NIR (near infrared)	$0.77\text{--}0.9$	[47]
NDMI	$(\text{NIR} - \text{SWIR1})/(\text{NIR} + \text{SWIR1})$	SWIR1 (shortwave infrared)	$1.55\text{--}1.75$	[31]

NDVI, Normalized Difference Vegetative Index; EVI, Enhanced Vegetative Index; MSAVI, Modified, Soil-Adjusted Vegetative Index; NDMI, Normalized Difference Moisture Index.  $G = 2$ ,  $C1 = 6$ ,  $C2 = 7.5$ ,  $L = 1$ .

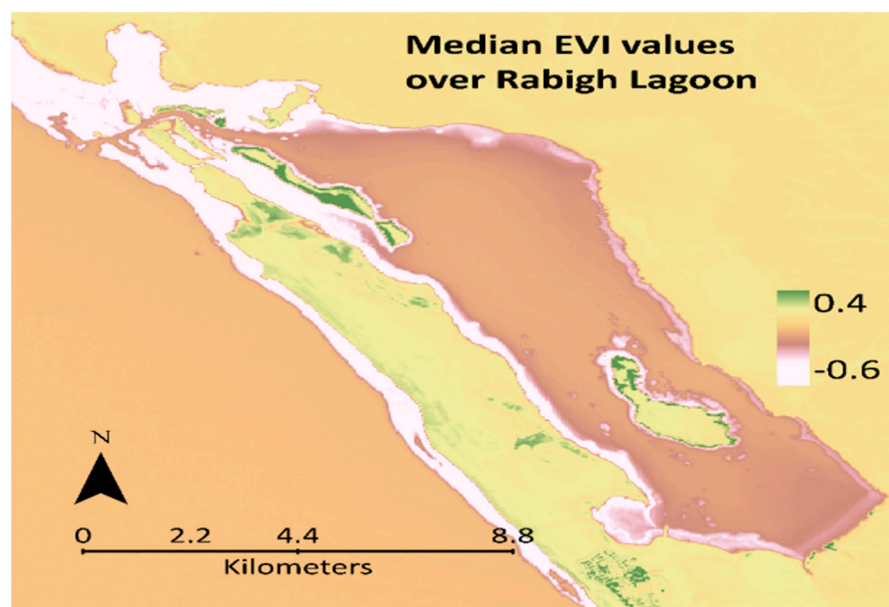


**Figure 2.** Median EVI over Rabigh Lagoon derived by calculating the median value using all the images between 1986 and 2019.

Workflow in Figure 3 shows how the images were processed and analyzed. Trend estimation was carried out on four (EVI, MSAVI, NDVI, and NDMI) annual raster time series covering the period of the last 34 years. Temporal changes in indices were interpreted as follows: increasing EVI, MSAVI, and NDVI meant the canopy is more productive (green) and in a healthy state. This is due to higher reflection of NIR (near infrared) by the spongy mesophyll of the all the leaves in the canopy and absorption of red wavelength by chloro-

phyll. In the case of NDMI, the SWIR1 reflection tells about the vegetation water content and spongy mesophyll structure. Higher water content would mean more absorption of SWIR1, thus leading to higher NDMI [48]. Slope of the yearly trend was calculated by linear least square regression where the index values act as response variable against the predictor variable, which in this case is time. Statistical significance of the regression coefficient was determined through Mann-Kendall trend test. The analysis was done using the “greenbrown” library [49] in RStudio (version 1.2.5033, Affero General Public License v3, Boston, MA, USA). The trend calculation algorithm in the “greenbrown” library offers the possibility to compute breaks in the time series by controlling the parameter  $h$ . Statistically, a breakpoint in the time series occurs when there is a structural change in the regression parameters before and after the break [50]. Ordinary Least Square Moving Sum (OLS-MOSUM) test is applied to detect whether any breaks exist in the time series. The detected break in a signal might depict an abrupt change such as clearcutting, logging, forest fire, landslide, and land management practices that might cause the index values to change with a large magnitude. However, breaks can also be induced by data artifacts [51]. For this study, the parameter  $h$ , which is the minimum time between detected breaks, was set to 5 years (0.15) for a 34-year time span. This means only the most significant abrupt change, if it exists, in the five-year period will be recorded. The regression analysis resulted in four trend maps showing areas with monotonic upward (greening) and downward (browning) patterns.

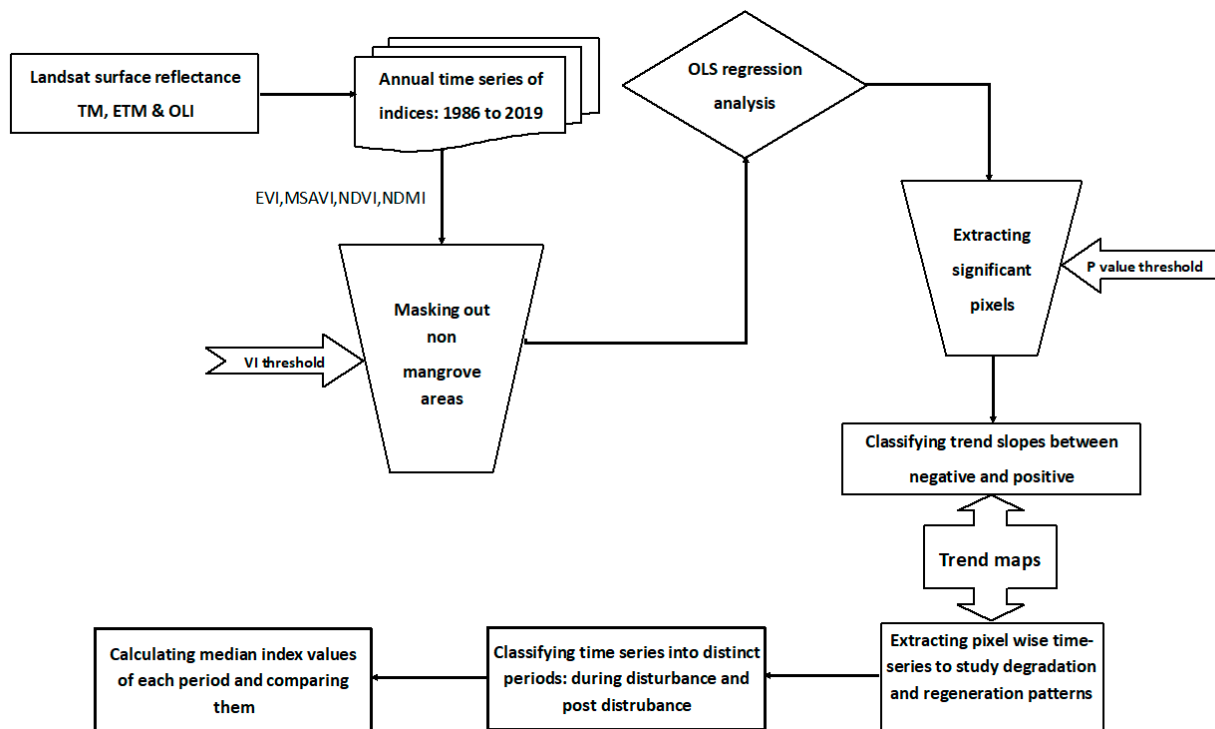


Figure 3. Framework for data acquisition and analysis.

All the spatial mapping was carried in ArcGIS Pro (version 2.6.3, Esri, Redlands, CA, USA). Using the trend maps, pixel-wise time series were extracted for each index and were analyzed as follows: to depict the health of mangroves, each time series was divided into two periods; during road obstruction (disturbed period) and after demolition of the road (recovery period). The disturbed period was represented by the years 1987 to 2012, whereas recovery period was represented by years 2013 to 2019. The median was calculated for each period per site and subsequently compared. If the difference between the median index values between the two periods was positive that was interpreted as recovery. Additionally, for easy comparison, the differences between disturbed and recovery periods

for all twelve sites were further averaged for each index. Similar calculations were made for the median of raster images. Kruskal-Wallis test was also performed in RStudio to identify any significant differences between the medians of both periods using median values for each site per index. Kruskal-Wallis is a non-parametric approach to detect any significant differences in a continuous dependent variable (median index values) against a categorical independent variable (period of disturbance and post disturbance recovery).

### 3. Results

Trend estimations from all four indices were analyzed for their spatial explicitness and temporal development. Figure 4 shows the spatial trend patterns computed by the regression algorithm. Only significant trends with  $p$ -values less than and equal to 0.05 (95% significance level) are shown. All trend slopes lie within the range of  $-0.01$  to  $0.01$ . Areas on trend maps (Figure 4) with bright orange/yellow to green colors indicate the range of weak positive ( $<0.01$ ) to strong positive ( $0.01$ ) trend, while areas with dark orange to red indicate the range for weak negative ( $<-0.01$ ) to strong negative trends ( $-0.01$ ). According to the histograms in Figure 5a–d, most pixels had a weak positive trend for all indices falling in the range of 0.001 to 0.005. MSAVI showed higher variation in the calculation of trend as can be seen by a greater number of bars. In addition to that, the number of pixels with significant positive trends (more than 0.001) was the highest for MSAVI (Figure 5b). This presents a good case for using MSAVI over regions with sparse vegetation since it can prevent the influence of background soil. The number of pixels with negative trends (slope value more than  $-0.001$ ) was highest for NDMI, indicating water-stressed mangroves (Figure 5d). The increasing trend shown in Figure 4 was mostly observed over natural areas with mangrove forests depicting subtle changes. The vegetation around Rabigh lagoon is dominated by mangrove trees [41]. Just near the coast, on the south west of the lagoon, there is a cluster of pixels with a strong positive trend over a region that has undergone modification and land use in terms of managed tree plantation on an area that was previously bare soil. Stronger greening patterns were observed for mangroves inside the lagoon compared to those for the mangroves just at the north western border of the lagoon. Of all four indices, the NDVI was the least reliable. Although overall patterns were similar, the NDVI does not perform well in sparsely vegetated areas, especially where highly heterogeneous pixels are influenced by surrounding bright soil.

Different plots (Figure 6) of calculated trend slopes for all four indices show correlation between EVI, MSAVI, NDVI, and NDMI and their statistical distribution. Overall correlation values between EVI, MSAVI, and NDVI are quite high, up to 0.98. On the other hand, lower values of correlation between NDMI with other indices were observed, with the maximum reaching up to 0.58. Nonetheless, all indices showed a dominant greening pattern. The box plots and QQ (quantile-quantile) plots show that all indices follow similar statistical distribution. The prominent presence of extreme values (especially positive) is indicated by data points falling on the line in the middle and deviating away from the line (above blue line for positive values and below blue line for negative values) forming heavy tails in the QQ plots. This is also reflected by the data points falling outside the upper and lower whisker in the box plot.

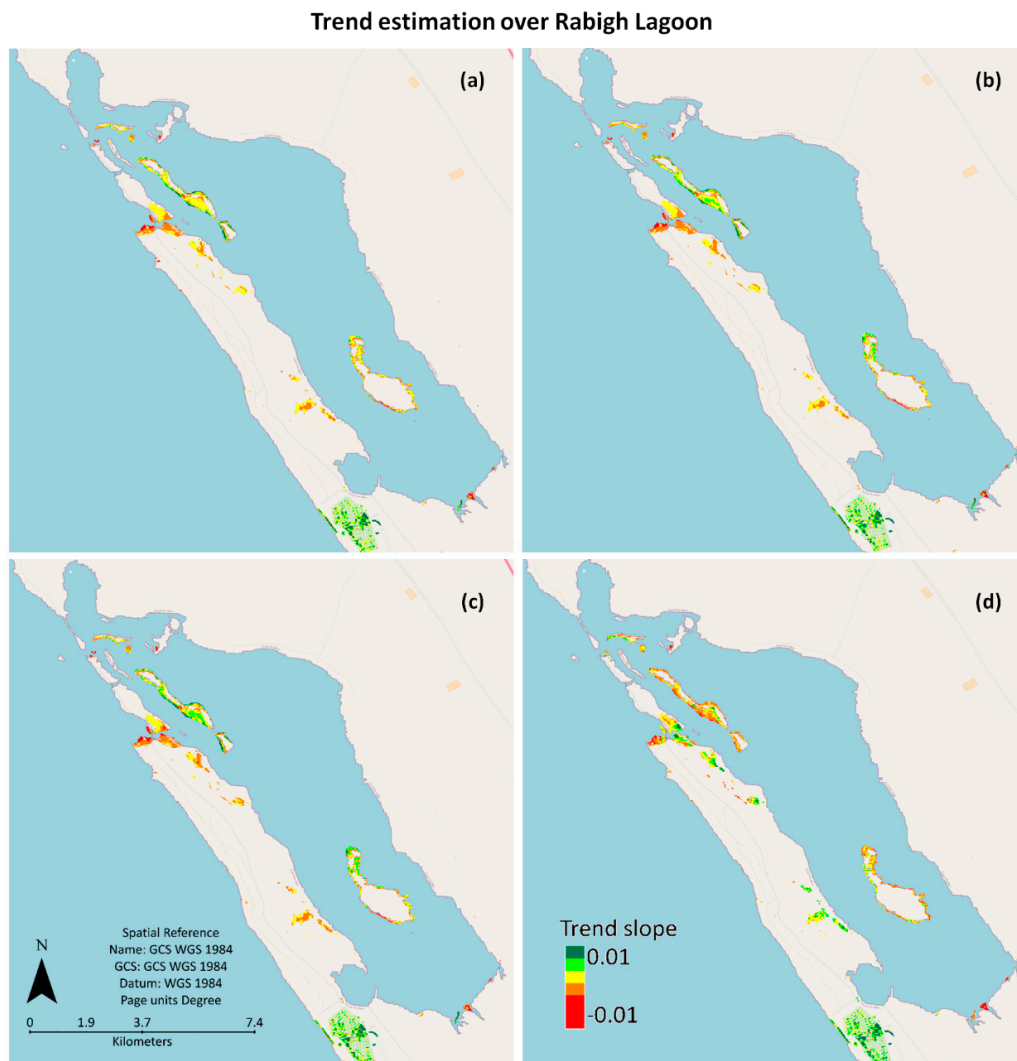


Figure 4. Regression slopes derived from the trend algorithm for (a) EVI, (b) MSAVI, (c) NDVI, and (d) NDMI.

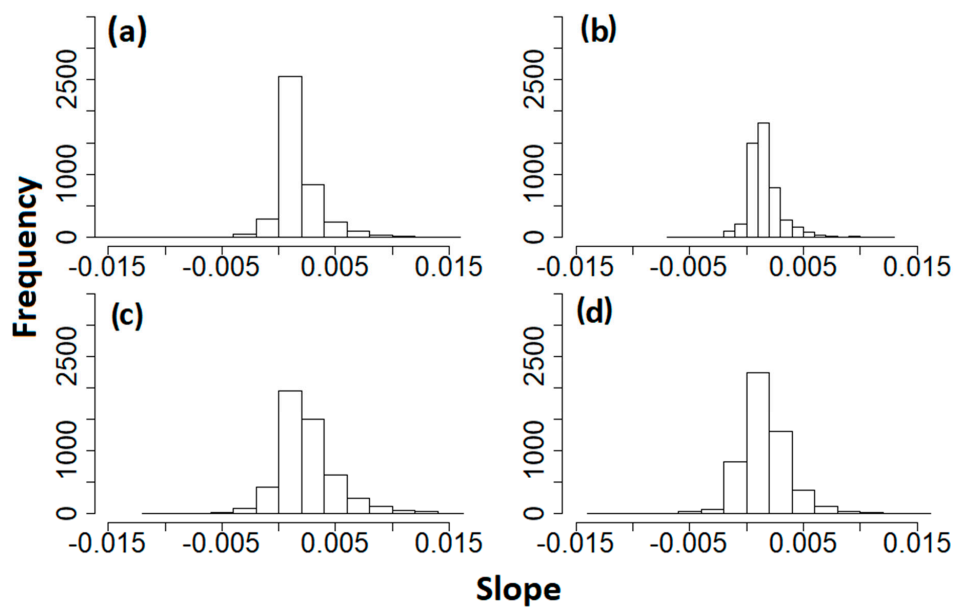
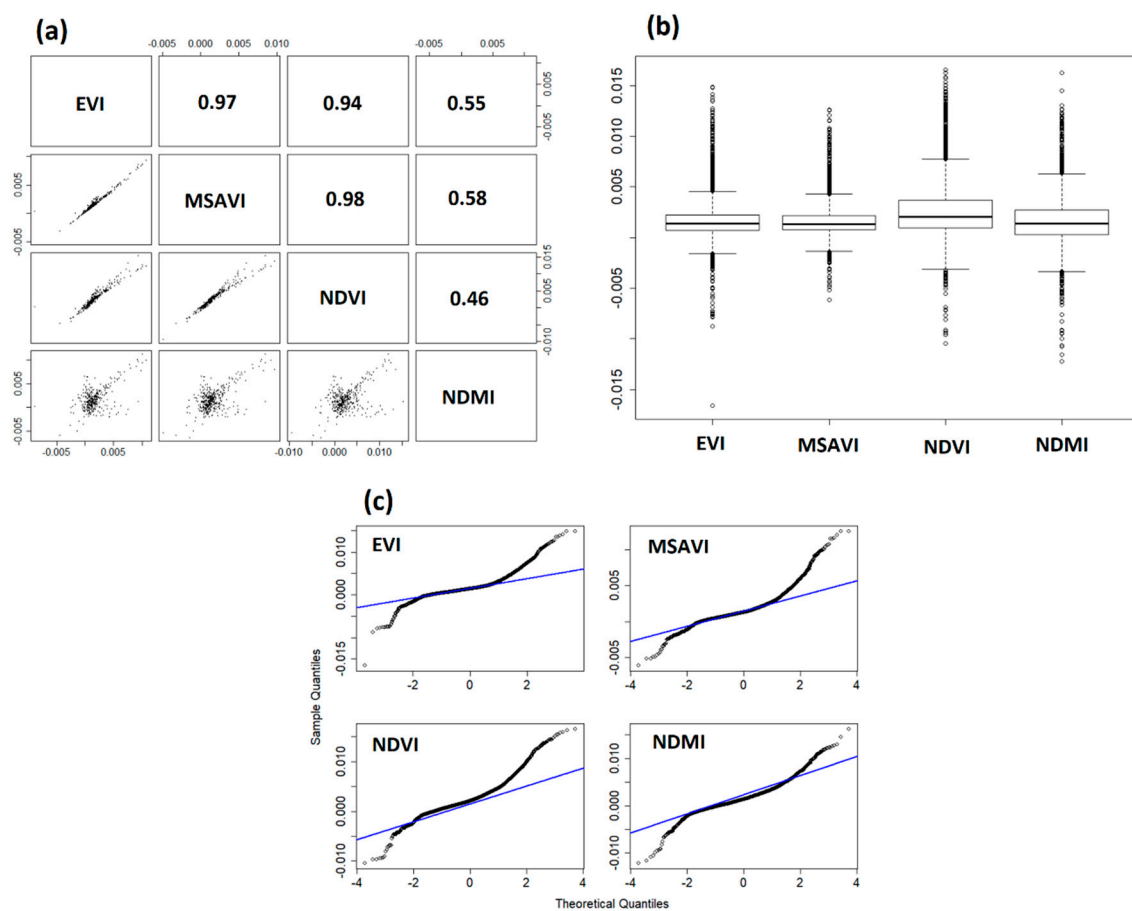
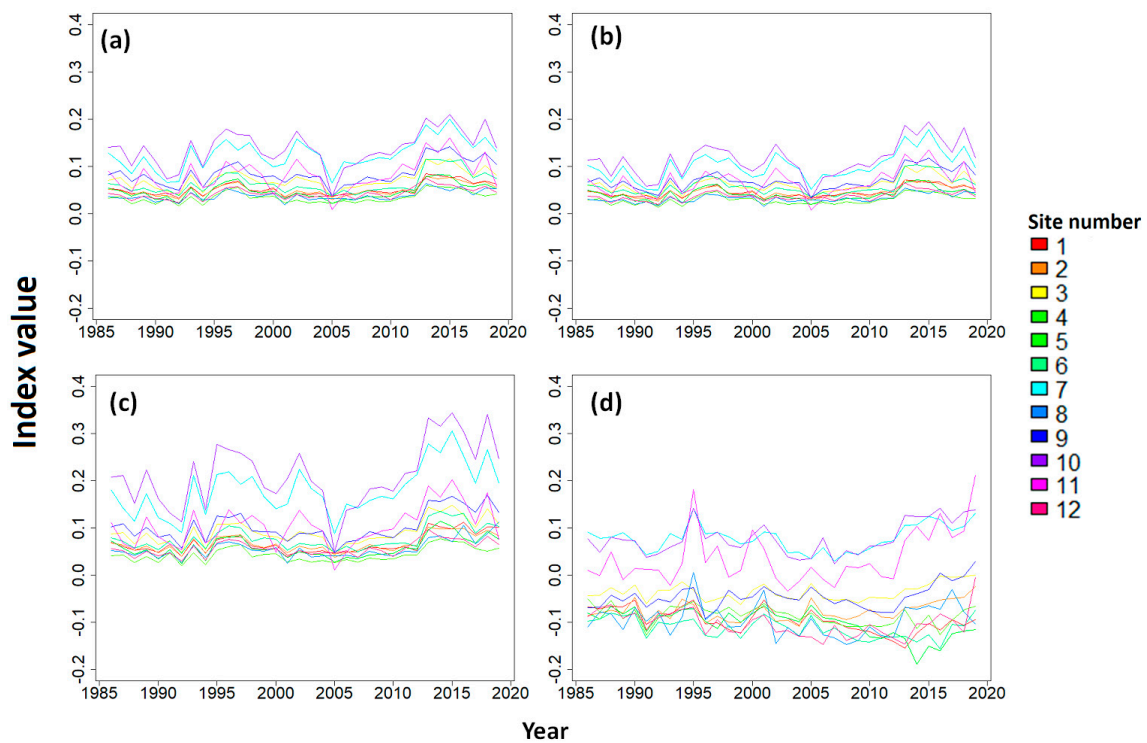


Figure 5. Histograms for trend slopes derived from (a) EVI, (b) MSAVI, (c) NDVI, and (d) NDMI.



**Figure 6.** Pair wise scatter plots (a), boxplot (b), and QQ (quantile-quantile) plots (c) showing the correlation and statistical distribution of trend slopes derived from EVI, MSAVI, NDVI, and NDMI.

Figure 7 shows the extracted time series over various sites with mangrove trees. A total of 12 time series were extracted. All the graphs show a very subtle development of index values. NDMI shows lower values than the other indices, which reflects water stress for plants largely triggered by obstructed water flow. For all indices, the end of time series can be seen showing higher values, and they stay above the values of those in the beginning of the time series (discussed further in Figure 8). That is why there is an observed monotonic upward trend. Low index values in 2005 were accounted for by the poor quality according to the “pixel quality assurance” band. Therefore, it was considered as noise. Outliers were considered as noise in this study. As long as noise did not result in break detection, cause regression parameters to be unstable, or lead to trend shifts, it was ignored from further investigation. In addition, any rise and fall in the signal between consecutive years was not interpreted as a trend because it was assumed that the mangrove ecosystem takes time to respond to external factors. Moreover, the lag period between the cause and effect has to be kept in mind when detecting vegetation response with satellite instruments. Local scale differences between the time series of the VIs (vegetation index) and moisture index can be attributed to the spectral differences where the VI used the IR (infrared) and visible (red and blue) part of the spectrum for highlighting the greenness of the vegetation. On the other hand, NDMI use only the infrared waves (IR and SWIR) characterizing the wetness of the vegetation.



**Figure 7.** Time series between 1986 and 2019 extracted from different mangrove sites (for all four indices: (a) EVI, (b) MSAVI, (c) NDVI, and (d) NDMI).

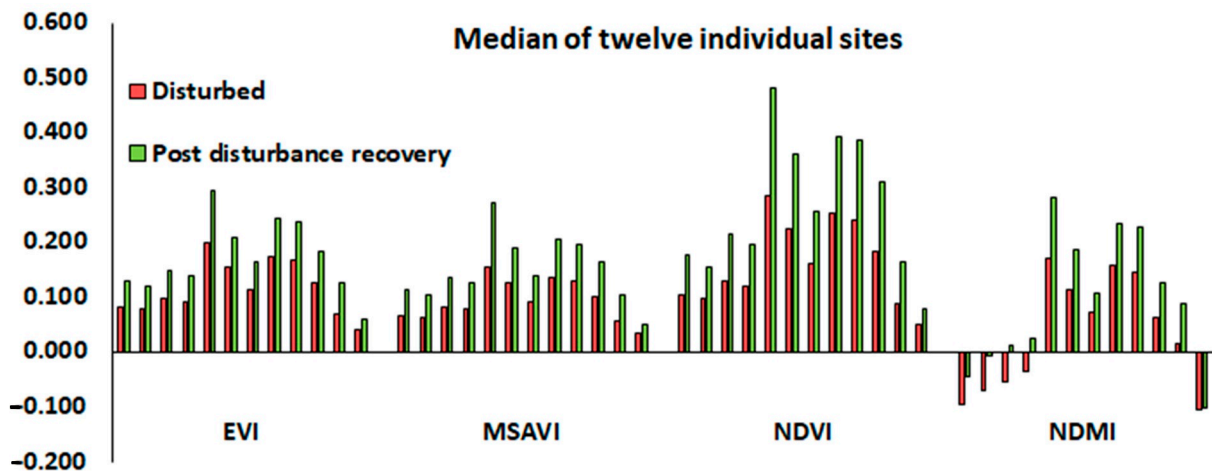


**Figure 8.** Median index values for disturbed and post disturbance recovery of mangroves for all twelve sites (Disturbance: 1987–2012, Recovery: 2013–2019).

In Figure 8, median values for each selected site can be seen changing during the two classified periods of time series. According to the output of Kruskal-Wallis test with  $p$ -value of 0.0006918 (against significance level of 0.05), there are significant differences in the median values of disturbance period from the recovery period. For all sites during the disturbance period (1987–2012), median values are lower, showing mangrove communities in an unhealthy state. Post disturbance (2013–2019), after demolishing the road, a gradual recovery of the mangroves was observed, which was reflected in the increased median index values compared to the values in disturbed state. Figure 9 shows the spatial pattern of median differences for the whole study site, which also came out to be positive. The average differences (Table 2) between the two periods were similar for EVI and MSAVI, whereas for NDVI, it was the highest. The NDVI usually shows higher values

because it tends to saturate over high biomass; therefore, the larger difference was not interpreted as a higher recovery. In the case of NDMI, the difference was only slightly larger than the difference of EVI and MSAVI. This could be a random occurrence. However, it is worthy to mention that NDMI is better at identifying forest disturbance and recovery because SWIR is more influenced by canopy moisture content [52]. For some sites ( $38.8361426^{\circ}$  E  $22.9962740^{\circ}$  N,  $38.9113980^{\circ}$  E  $22.8789328^{\circ}$  N,  $38.9140997^{\circ}$  E  $22.8773751^{\circ}$  N), NDMI shows negative values even in the recovery period, which could mean higher water stress. In addition, negative NDMI values also mean low canopy cover, which was illustrated by visualizing high-resolution Google Earth imagery.

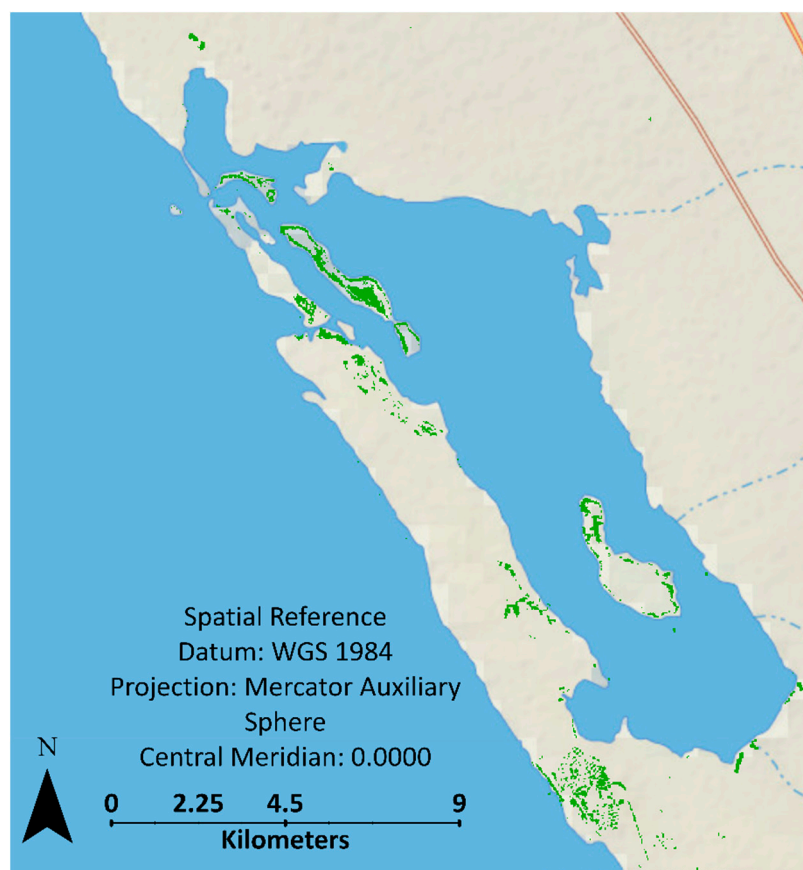


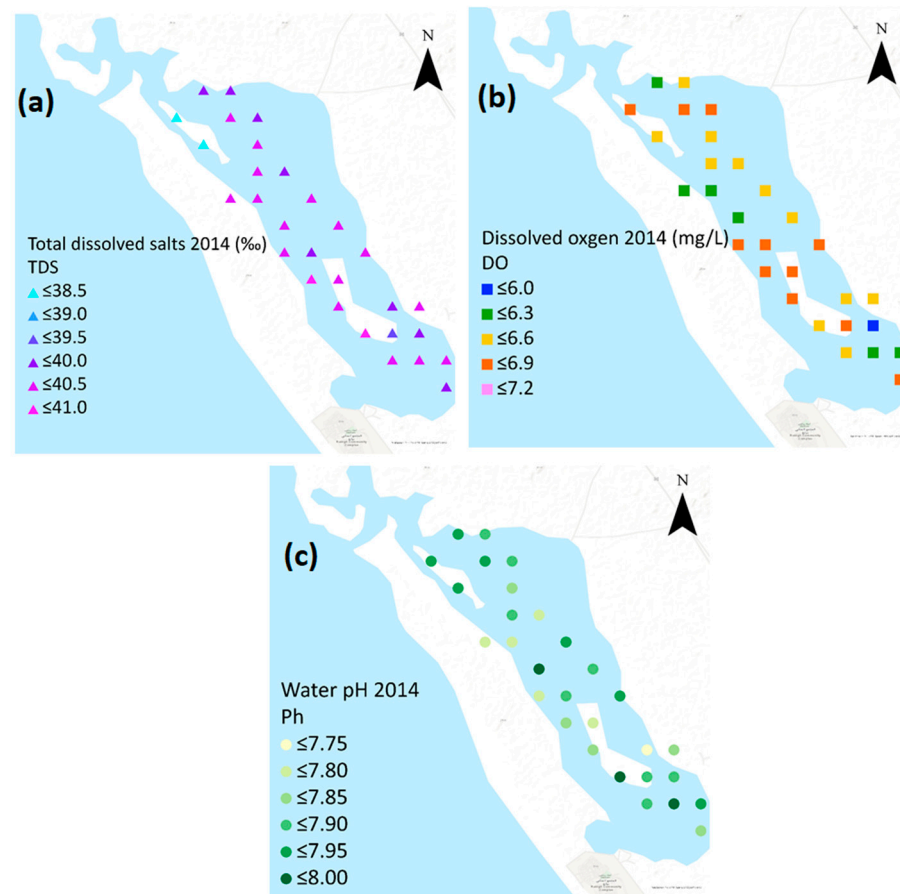
Figure 9. Spatial pattern of post disturbance recovery (show in green).

Table 2. Averaged median values of disturbed and recovery period and their difference.

Index	Disturbance	Recovery	Difference
EVI	0.104	0.155	0.052
MSAVI	0.086	0.136	0.051
NDVI	0.143	0.235	0.092
NDMI	0.038	0.096	0.066

This study relates degradation and recovery patterns in response to obstructed water recharge, resulting in disturbed levels of salinity, dissolved oxygen, and pH. Tidal and water chemistry are two main parameters considered to effect mangrove productivity [53]. Therefore, it is helpful to consider these factors when interpreting trend patterns. Under higher-salinity and low-nutrient conditions, mangroves increase the process of transpiration to excrete the salt, which could lead to less growth or productivity. Figure 10 shows the aforementioned parameters of the lagoon for the year 2014. The data were taken from the study of Youssef and Sorogy [54] and mapped to visualize the spatial pattern. Since no

such data are available during the disturbance period, a direct comparison cannot be made. Nevertheless, values in Figure 10 do suggest that mangroves are returning to a healthy state because the parameters in the surrounding lagoon water are within the normal range (mangroves in Rabigh are acclimatized to 40 ppt salinity) [20].



**Figure 10.** Surface water parameters (a) salinity or dissolved salts, (b) dissolved oxygen and (c) pH. The sampling and estimation was done in 2014 [55].

Rainfall and temperature data, provided by CRUTS (Climate Research Unit gridded Time Series), were also used to assess their impact on degradation and regeneration patterns. The data were produced through the interpolation of observations from weather stations. Monthly data was downloaded, and the trend was estimated through linear least square regression on annually aggregated series against a 95% significance level. According to Figure 11, an increasing trend in temperature and non-significant trend in precipitation was observed. Whereas it could be contemplated that a combination of both climatic parameters could have had an influence on mangroves, this cause-and-effect relation must be proceeded on with extreme caution. Firstly, the data had a very coarse spatial resolution. For pixel-to-pixel correlation, climatic and index data must be of the same spatial resolution. Rainfall and temperature were recorded from the monitoring station in Jeddah that is at a distance of 141 km from Rabigh. While such datasets might be useful to monitor the impacts of major climatic events and general trend patterns in the context of globally rising temperatures, it might not always be helpful in reflecting a spatially and temporally explicit situation. This is especially the case where a combination (multivariate) of factors have a nonlinear effect and linear statistical correlations might not be enough.

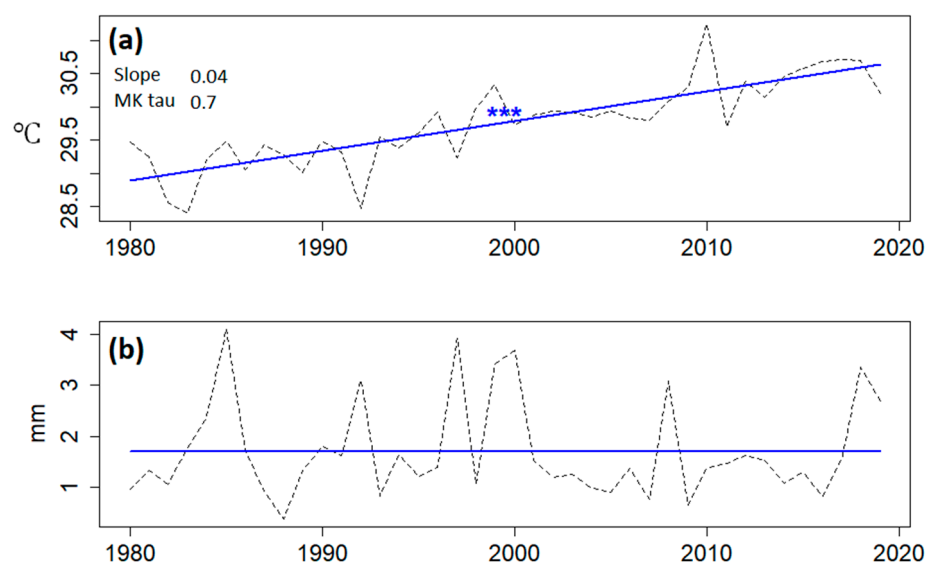


**Figure 11.** Trend (blue line) analysis for annual average (a) temperature and (b) rainfall. Trend for rainfall came out to be non-significant, therefore slope and MK (Mann-Kendall) tau values are not shown. The symbol \* shows the trend is significant, with three \* meaning highly significant having  $p$  value of less than 0.000001.

#### 4. Discussion

The deterioration of mangrove species has been observed at a regional and global scale. According to Al Shiekh [55], there has been a loss of 46% of vegetation cover between 1987 and 2002 in the Red Sea coast at the Jazan region, Saudi Arabia. The reasons discussed for this loss are demographic growth and aquaculture. On the contrary, a recent study by Almahasheer et al. [33] reported an expansion of 12% in mangrove area along the Red Sea. This expansion was observed over 41 years from 1972 to 2013 based on multi-temporal Landsat data analysis. Although our study investigated only a small part of the Red Sea, it does correlate with the findings of Almahasheer et al. [33] such that our study showed a monotonic upward trend for mangroves in the form of regeneration after the road in the north west of the lagoon was dismantled. Our study used the approach of “intercomparison” for indirect validation of the observed trends. Intercomparison involves [56] using multiple data products to draw out simplified estimations of major spatial and temporal patterns. The multiple data products in this study were the four indices using different band combination to assess the temporal change in the spectral response.

Mangroves show a lot of tolerance to various stress factors they are exposed to [57]. The generated time series (Figure 7) of annual records of EVI, MSAVI, NDVI, and NDMI over twelve sites of mangrove habitats in the Rabigh lagoon from 1986 to 2019 showed an interesting pattern of ecological dynamics of mangrove population. There are very subtle changes taking place in the region, where at some sites, mangroves tend to be stable through a loss and gain strategy, and at others, they show a declining tendency. According to Vovides et al. [58], mangrove regeneration post disturbance in arid and semi-arid regions could prove to be a challenge. This is especially the case where plantation activities alone, without eliminating the stress factor, will not bring desired results. Twilley et al. [59] investigated similar hydrological stress on mangroves in CGSM lagoon (Cienaga Grande de Santa Marta) Colombia, brought on by coastal highway construction. The authors highlighted that the recovery rate of the mangrove wetlands depends on the intensity and persistence of the disturbance, type and age of species, and natural tree mortality, where adult trees after dying leave gaps in the canopy giving space for new seedlings to grow. Based on the study of Twilley et al. [59], natural hydrological restoration and mangrove plantations were the main assessed factors important for mangrove recovery.

In the region of Rabigh, the prominent limiting factors for mangrove growth are optimum hydrological conditions in the form of mainly water circulation from the open sea and limited rainfall. A sand pathway, hindering water circulation, has been present between 1987 and 2012. Since mangrove forests are wetlands and have a deep root system, persistent water obstruction may take a few years to have a prolonged and visible (such as stunted growth and yellowing of leaves) and detectable impact on mangrove's health [60]. This is so because mangrove roots are efficient in absorbing water from sediments. Moreover, since Rabigh Lagoon is surrounded by inland desert, mangrove species there are adapted to dry and warm conditions and will show resilience to drought-like conditions. It should be kept in mind though that at the physiological level, degradation might be immediately detected. The lag discussed in this paper is solely in terms of the satellite detection of vegetation status when viewing the canopy greenness and wetness. The sand passageway was partly flooded by water in 1990, after which the lagoon was connected to the sea through manually laid downpipes (Figure 12). With the passage of time, these pipes were blocked by sedimentation. As a result, there was a slow and reduced water re-charge into the lagoon. During this period, the mangroves were gradually recovering while the degradation processes were still active.



**Figure 12.** Pipes laid down under the sand passage to allow water circulation.

In 2012, the sand passageway was completely demolished, and the lagoon was re-connected with the open sea. As a result, there was unobstructed natural water circulation and also an increased nutrient supply. This is reflected by increasing index values for all indices in all twelve sites, especially from 2013 onward where the values are the highest during the whole evaluation period. Three sites in particular were visited as part of an ongoing project in Rabigh Lagoon since the 1990s and therefore are presented as case studies in the following sections. Figures 13–15 show results from pixel-based trend analysis for EVI, MSAVI, NDVI, and NDMI for the three locations. They are further discussed below. All three sites present a case study of disturbance (due to road construction) and recovery after the road was demolished and the effect of various stress factors was diminished.

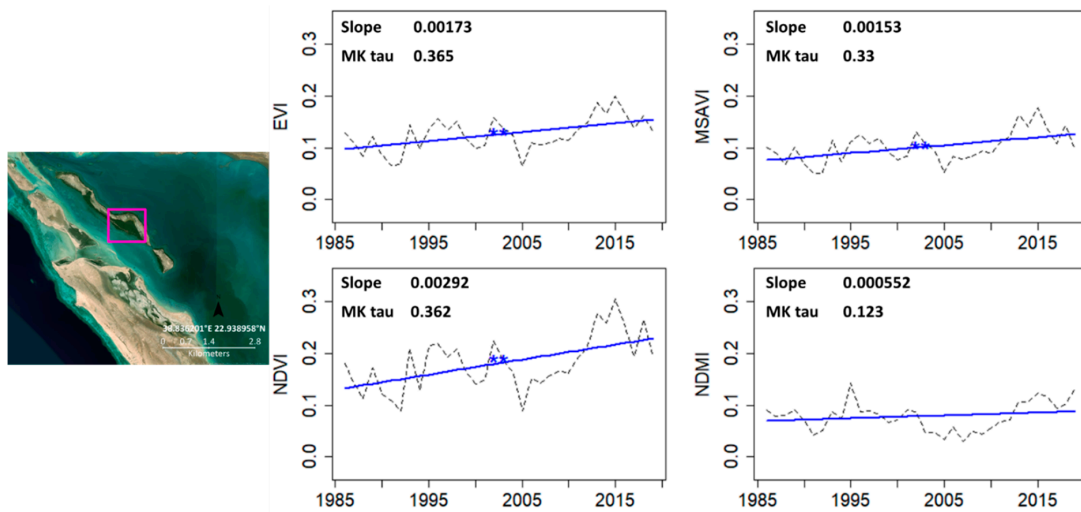


**Figure 13.** Trend (blue line) analysis for site in the north (enclosed in pink box). The symbol \* shows the trend is significant, with two \* meaning  $p$  value of equal or less than 0.001.

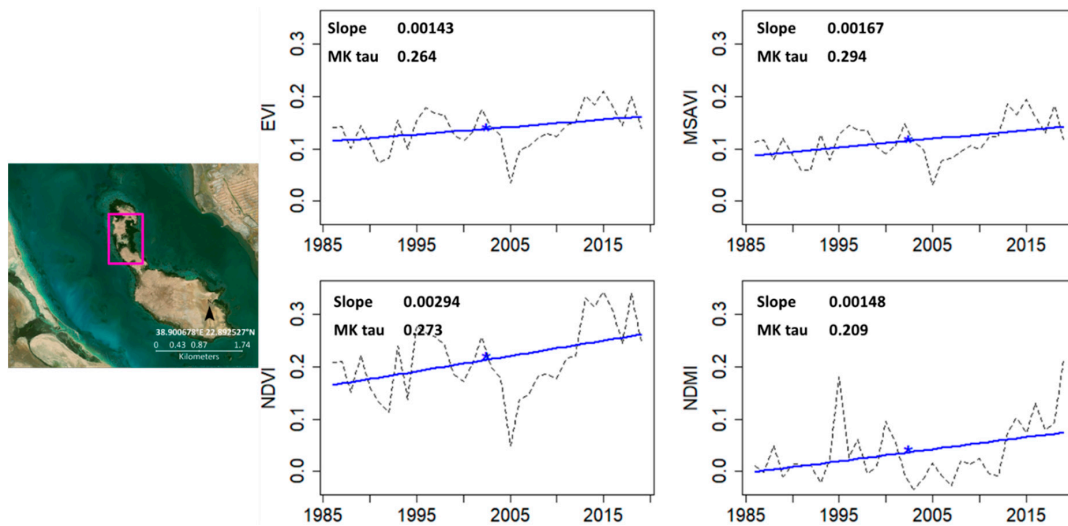


**Figure 14.** Trend (blue line) analysis for site in the south (enclosed in pink box). The symbol \* shows the trend is significant, with one \* meaning  $p$  value of equal or less than 0.05.

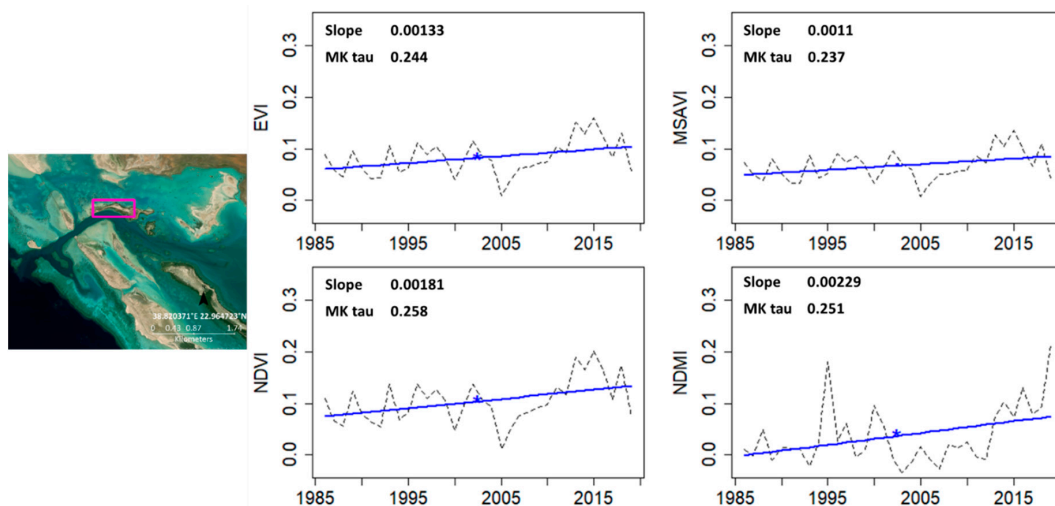


**Figure 15.** Trend (blue line) analysis for site in extreme northwest (enclosed in pink box). The symbol \* shows the trend is significant, with one \* meaning  $p$  value of equal or less than 0.05.

#### 4.1. North of Lagoon

This site, as shown in Figure 13, is in the northern part of the lagoon facing a skewed, deep entrance to the open sea. Due to this, only the tiny deep channel allows water circulation between the lagoon and the open sea. The habitat at this location is mixed between coral reefs and mangroves. Mangroves are scattered in patches. This area has suffered from extreme wind and tides that led to massive erosion; therefore, mangrove trees were under high environmental stress. Slope values for EVI, MSAVI, and NDVI range from 0.0015 to 0.003. The MK (Mann-Kendall) tau correlation coefficient came out to be the highest for EVI, MSAVI, and NDVI, which meant that around 35% variability in VI is explained by time. However, in the case of NDMI, low tau and slope values indicate a weak relation between trend and time and weak trend, respectively. This could indicate that the moisture content of mangroves at this particular location might not be a driving factor for degradation and recovery patterns as much as chlorophyll content is. No breaks were detected, which means there has been a gradual upward trend.

#### 4.2. South of Lagoon

This site is present in the second island toward the southern part of the lagoon where freshwater flow is mainly supplied by rain and flood. According to Figure 14, the slope values lie between 0.0015 and 0.003. Only gradual change was observed. MK tau values showed that 20% to 30% variation in index values was explained by time. This site was under sedimentation process, receiving more mud and clay from runoff. The increase of sedimentary conditions may have affected water circulation and increased the deposition of organic matter causing lower index values during the disturbance period.

#### 4.3. Extreme Northwest of Lagoon

Located in the Camel Island facing the third entrance of water, it is relatively a small channel. It can be seen from Figure 15 that no abrupt changes were detected by the regression algorithm. At low tide, camels used to cross the shallow water toward the island for grazing. This site has suffered the most degradation, as the index values are lower compared to the other two sites. The calculated trend for EVI, MSAVI, and NDVI was in the range of 0.001. On the contrary, slope value (0.002) and tau value (25%) were the highest for NDMI for this site, suggesting that moisture was the dominant limiting factor. Figure 16 shows photos taken from the field visit conducted at this particular location during various stages of an ongoing project. The temporal variability of mangrove vegetation can be visualized; there is evident degradation in the 1990s followed by a return to a healthy state after natural water flow was resumed.

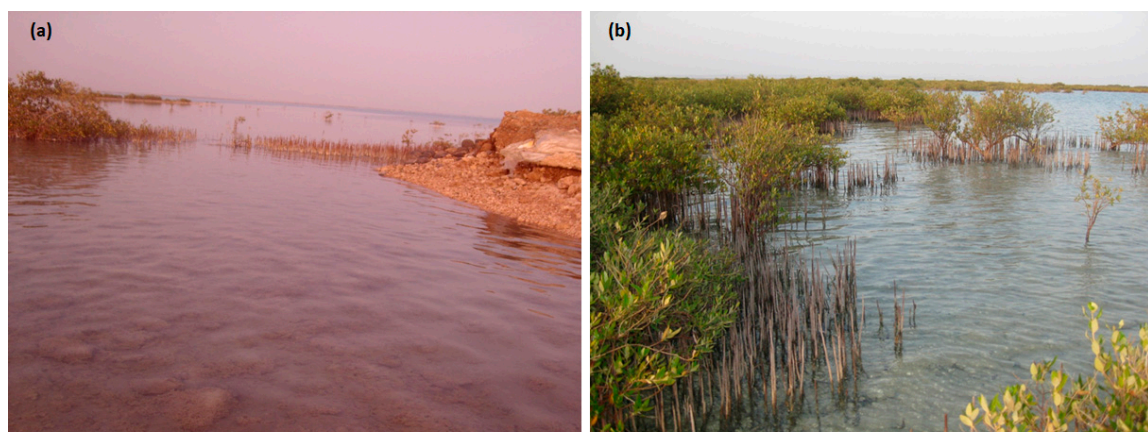


**Figure 16.** Photos from field visits: (a) 1993 showing disturbed mangroves and (b) 2019 showing recovering mangroves at site in extreme northwest.

For all three sites, no breaks were found as result of abrupt changes in the index values. This indicates there is no clearcutting and large-scale urbanization that would cause a sudden drop in the index value with at least a change in magnitude exceeding 0.2 units. Mostly the changes are subtle and persistent. That is why despite the curve having a period of low values, the slope line shows up as a long-term pattern of increasing trend. This study only investigated EVI, MSAVI, NDVI, and NDMI as an indicator for mangrove disturbance and recovery. Other parameters such as water salinity gradients, dissolved oxygen, and other water quality parameters could not be analyzed with the same temporal frequency as the indices. A change in population or community structure occurring at the boundaries of habitats is also an essential aspect that is difficult to monitor with medium-resolution imagery. Additionally noteworthy here is the influence of marine erosion on the stability of mangroves, especially for smaller patches of mangroves, as is the case for Rabigh. It is suggested to consider these additional drivers in future studies regarding mangroves of the Red Sea and particularly in the area of Rabigh lagoon. In addition, to better understand vegetation recovery, experimental setups or projects involving mangrove restoration could be devised to study and prioritize drivers essential for regeneration processes.

## 5. Conclusions

This study attempted to monitor mangrove disturbance and the post-disturbance recovery pattern in Rabigh lagoon along the coast of the Red Sea through trend analysis of various indices. Moreover, observed patterns were analyzed in the context of road construction that hindered water circulation through the lagoon. Our aim was to capture long-lived processes as opposed to temporary and short-lived changes. The outcome of this study showed that time series analysis of selected vegetation and moisture indices (EVI, MSAVI, NDVI and NDMI) was able to capture a pattern of disturbance and recovery. Even if the changes were gradual, they could still be identified. It is suggested to use MSAVI and NDMI to assess ecological disturbance and recovery, particularly for sparsely vegetated and arid areas. However, validating observed patterns using only the regression slope proved to be a challenge. This is so because the response of a natural ecosystem to gradual changes is complex. Integrating rain and temperature data in our interpretation scheme was only partially helpful, as it aided in explaining general patterns, but climatic anomalies were not able to account for extreme values in the index time series. Future studies must integrate the estimation of surface water parameters at constant time intervals to relate various stress factors with mangrove response. Furthermore, extensive and regular field visits to visualize the condition of mangrove stands could also help validate the observed patterns.

**Author Contributions:** Conceptualization, M.O.A. and W.R.K.; methodology, W.R.K. and S.M.; formal analysis, S.M.; data, S.M.; writing—original draft preparation, M.O.A. and W.R.K.; writing—review and editing, S.M.; visualization, M.O.A.; project administration, M.O.A.; funding acquisition, M.O.A. All authors have read and agreed to the published version of the manuscript.

**Funding:** This project was funded by the National Plan for Science, Technology, and Innovation (MAARIFAH), King Abdulaziz City for Science and Technology, the Kingdom of Saudi Arabia (award number 14-ENV263-03).

**Acknowledgments:** This project was funded by the National Plan for Science, Technology, and Innovation (MAARIFAH), King Abdulaziz City for Science and Technology, the Kingdom of Saudi Arabia (award number 14-ENV263-03). The authors also acknowledge with thanks the Science and Technology Unit, King Abdulaziz University for technical support.

**Conflicts of Interest:** The authors declare no conflict of interest.

## References

- Guangyi, Z. Influences of tropical forest changes on environmental quality in Hainan province, PR of China. *Ecol. Eng.* **1995**, *4*, 223–229. [[CrossRef](#)]
- Costanza, R.; d'Arge, R.; De Groot, R.; Farber, S.; Grasso, M.; Hannon, B.; Limburg, K.; Naeem, S.; O'Neill, R.V.; Paruelo, J. The value of the world's ecosystem services and natural capital. *Nature* **1997**, *387*, 253–260. [[CrossRef](#)]
- Khan, W.R.; Nazre, M.; Zulkifli, S.Z.; Kudus, K.A.; Zimmer, M.; Roslan, M.K.; Mukhtar, A.; Mostapa, R.; Gandaseca, S. Reflection of stable isotopes and selected elements with the inundation gradient at the Matang Mangrove Forest Reserve (MMFR), Malaysia. *Int. For. Rev.* **2017**, *19*, 1–10. [[CrossRef](#)]
- Lee, H.-Y.; Shih, S.-S. Impacts of vegetation changes on the hydraulic and sediment transport characteristics in Guandu mangrove wetland. *Ecol. Eng.* **2004**, *23*, 85–94. [[CrossRef](#)]
- Lewis, R.R., III. Ecological engineering for successful management and restoration of mangrove forests. *Ecol. Eng.* **2005**, *24*, 403–418. [[CrossRef](#)]
- Willis, J.M.; Hester, M.W.; Shaffer, G.P. A mesocosm evaluation of processed drill cuttings for wetland restoration. *Ecol. Eng.* **2005**, *25*, 41–50. [[CrossRef](#)]
- Sánchez-Carrillo, S.; Sánchez-Andrés, R.; Alatorre, L.C.; Angeler, D.G.; Álvarez-Cobelas, M.; Arreola-Lizárraga, J.A. Nutrient fluxes in a semi-arid microtidal mangrove wetland in the Gulf of California. *Estuar. Coast. Shelf Sci.* **2009**, *82*, 654–662. [[CrossRef](#)]
- Fickert, T. To Plant or Not to Plant, That Is the Question: Reforestation vs. Natural Regeneration of Hurricane-Disturbed Mangrove Forests in Guanaja (Honduras). *Forests* **2020**, *11*, 1068. [[CrossRef](#)]
- Khan, W.R.; Rasheed, F.; Zulkifli, S.Z.; Kasim, M.R.B.M.; Zimmer, M.; Pazi, A.M.; Kamrudin, N.A.; Zafar, Z.; Faridah-Hanum, I.; Nazre, M. Phytoextraction Potential of *Rhizophora Apiculata*: A Case Study in Matang Mangrove Forest Reserve, Malaysia. *Trop. Conserv. Sci.* **2020**, *13*, 1940082920947344. [[CrossRef](#)]
- Kathiresan, K.; Bingham, B.L. Biology of mangroves and mangrove ecosystems. *Adv. Mar. Biol.* **2001**, *40*, 84–254.
- Spalding, M.; Blasco, F.; Field, C. *World Mangrove Atlas*; International Society for Mangrove Ecosystems: Okinawa, Japan, 1997. Available online: [www.environmentalunit.com/Documentation/04%20Resources%20at%20Risk/World%20mangrove%20atlas.pdf](http://www.environmentalunit.com/Documentation/04%20Resources%20at%20Risk/World%20mangrove%20atlas.pdf) (accessed on 15 October 2020).
- Dahdouh-Guebas, F.; Mathenge, C.; Kairo, J.G.; Koedam, N. Utilization of mangrove wood products around Mida Creek (Kenya) amongst subsistence and commercial users. *Econ. Bot.* **2000**, *54*, 513–527. [[CrossRef](#)]
- Ruiz-Luna, A.; Berlanga-Robles, C.A. Land use, land cover changes and coastal lagoon surface reduction associated with urban growth in northwest Mexico. *Landsc. Ecol.* **2003**, *18*, 159–171. [[CrossRef](#)]
- Ruiz-Luna, A.; Acosta-Velázquez, J.; Berlanga-Robles, C.A. On the reliability of the data of the extent of mangroves: A case study in Mexico. *Ocean Coast. Manag.* **2008**, *51*, 342–351. [[CrossRef](#)]
- Saenger, P.; Khalil, A.S.M. Regional Action Plan for the Conservation of Mangroves. In *PERGA/GEF Regional Action Plan for the Conservation of Marine Turtles, Seabirds and Mangroves in the Red Sea and Gulf of Aden*; Technical Series 12; PERSGA: Jeddah, Saudi Arabia, 2007; pp. 101–129.
- Khalil, A.S.M.; Krupp, F. Fishes of the mangrove ecosystem. In *Comparative Ecological Analysis of Biota and Habitats in Littoral and Shallow Sublittoral Waters of the Sudanese Red Sea*; Report for the Period of Apr 1991–Dec 1993; Faculty of Marine Science and Fisheries, Port Sudan, and Forschungsinstitut Senckenberg: Frankfurt, Germany, 1994.
- Wilkie, M.L. *Mangrove Conservation and Management in the Sudan*; Consultancy Report. Based on the Work of Ministry of Environment and Tourism. FOL/CF Sudan. FP:GCP/SUD/O47/NET; FAO: Khartoum, Sudan, 1995; 92p.
- Ormond, R.F.G. Management and conservation of Red Sea habitats. In *The coastal and marine environments of the Red Sea, Gulf of Aden and Tropical Western Indian Ocean. Proceedings of Symposium, Khartoum (January). The Red Sea and the Gulf of Aden Environmental Programme Jeddah*; 1980; Volume 2, pp. 135–162. Available online: [http://www.reefbase.org/resource\\_center/publication/pub\\_4287.aspx](http://www.reefbase.org/resource_center/publication/pub_4287.aspx) (accessed on 15 October 2020).
- Mandura, A.S. A mangrove stand under sewage pollution stress: Red Sea. *Mangroves Salt Marshes* **1997**, *1*, 255–262. [[CrossRef](#)]
- Raitsos, D.E.; Hoteit, I.; Prihartato, P.K.; Chronis, T.; Triantafyllou, G.; Abualnaja, Y. Abrupt warming of the Red Sea. *Geophys. Res. Lett.* **2011**, *38*. [[CrossRef](#)]
- Rasolofoharino, M.; Blasco, F.; Bellan, M.F.; Aizpuru, M.; Gauquelin, T.; Denis, J. A remote sensing based methodology for mangrove studies in Madagascar. *Int. J. Remote Sens.* **1998**, *19*, 1873–1886. [[CrossRef](#)]
- Gao, J. A comparative study on spatial and spectral resolutions of satellite data in mapping mangrove forests. *Int. J. Remote Sens.* **1999**, *20*, 2823–2833. [[CrossRef](#)]
- Blasco, F.; Aizpuru, M. Mangroves along the coastal stretch of the Bay of Bengal: Present status. *Ind. J. Mar. Sci.* **2002**, *31*, 9–20.
- Saito, H.; Bellan, M.F.; Al-Habshi, A.; Aizpuru, M.; Blasco, F. Mangrove research and coastal ecosystem studies with SPOT-4 HRVIR and TERRA ASTER in the Arabian Gulf. *Int. J. Remote Sens.* **2003**, *24*, 4073–4092. [[CrossRef](#)]
- Alatorre, L.C.; Sánchez-Andrés, R.; Cirujano, S.; Beguería, S.; Sánchez-Carrillo, S. Identification of mangrove areas by remote sensing: The ROC curve technique applied to the northwestern Mexico coastal zone using Landsat imagery. *Remote Sens.* **2011**, *3*, 1568–1583. [[CrossRef](#)]
- Jensen, J.R.; Lin, H.; Yang, X.; Ramsey, E., III; Davis, B.A.; Thoenke, C.W. The measurement of mangrove characteristics in southwest Florida using SPOT multispectral data. *Geocarto Int.* **1991**, *6*, 13–21. [[CrossRef](#)]

27. Ramsey, E.W., III; Jensen, J.R. Remote sensing of mangrove wetlands: Relating canopy spectra to site-specific data. *Photogramm. Eng. Remote Sens.* **1996**, *62*, 939–948.
28. Green, E.P.; Mumby, P.J.; Edwards, A.J.; Clark, C.D.; Ellis, A.C. Estimating leaf area index of mangroves from satellite data. *Aquat. Bot.* **1997**, *58*, 11–19. [[CrossRef](#)]
29. Green, E.P.; Clark, C.D.; Mumby, P.J.; Edwards, A.J.; Ellis, A.C. Remote sensing techniques for mangrove mapping. *Int. J. Remote Sens.* **1998**, *19*, 935–956. [[CrossRef](#)]
30. Green, E.; Mumby, P.; Edwards, A.; Clark, C. *Remote Sensing: Handbook for Tropical Coastal Management*; United Nations Educational, Scientific and Cultural Organization (UNESCO): Paris, France, 2000.
31. Huete, A.; Didan, K.; Miura, T.; Rodriguez, E.P.; Gao, X.; Ferreira, L.G. Overview of the radiometric and biophysical performance of the MODIS vegetation indices. *Remote Sens. Environ.* **2002**, *83*, 195–213. [[CrossRef](#)]
32. Gao, B.-C. NDWI—A normalized difference water index for remote sensing of vegetation liquid water from space. *Remote Sens. Environ.* **1996**, *58*, 257–266. [[CrossRef](#)]
33. Almahasheer, H.; Aljowair, A.; Duarte, C.M.; Irigoien, X. Decadal stability of Red Sea mangroves. *Estuar. Coast. Shelf Sci.* **2016**, *169*, 164–172. [[CrossRef](#)]
34. Elsebaie, I.H.; Aguib, A.S.H.; Al Garni, D. The Role of Remote Sensing and GIS for Locating Suitable Mangrove Plantation Sites Along the Southern Saudi Arabian Red Sea. *Int. J. Geosci.* **2013**, *4*, 471–479. [[CrossRef](#)]
35. Kumar, A.; Khan, M.A.; Muqtadir, A. Distribution of mangroves along the Red Sea coast of the Arabian Peninsula: Part-I: The northern coast of western Saudi Arabia. *Earth Sci. India* **2010**, *3*.
36. Abd-El Monsef, H.; Smith, S.E. A new approach for estimating mangrove canopy cover using Landsat 8 imagery. *Comput. Electron. Agric.* **2017**, *135*, 183–194. [[CrossRef](#)]
37. Braithwaite, C.J.R. *Geology and Palaeogeography of the Red Sea Region*; Edwards, A.J., Head, S.M., Eds.; Red Sea (Key Environments); Pergamon Press: Oxford, UK, 1987; pp. 22–44.
38. Brown, G.F.; Schmidt, D.L.; Huffman, A.C., Jr. *Geology of the Arabian Peninsula*; Shield Area of Western Saudi Arabia (No. 560-A); US Geological Survey: Reston, VA, USA, 1989; 188p.
39. Al-Washmi, H.A. Sedimentological aspects and environmental conditions recognized from the bottom sediments of Al-Kharrar Lagoon, eastern Red Sea coastal plain, Saudi Arabia. *J. KAU Mar. Sci.* **1999**, *10*, 71–87. [[CrossRef](#)]
40. Al-Dubai, T.A.; Abu-Zied, R.H.; Basaham, A.S. Present environmental status of Al-Kharrar Lagoon, central of the eastern Red Sea coast, Saudi Arabia. *Arab. J. Geosci.* **2017**, *10*, 305. [[CrossRef](#)]
41. Aljahdali, M.O.; Alhassan, A.B. Ecological risk assessment of heavy metal contamination in mangrove habitats, using biochemical markers and pollution indices: A case study of *Avicennia marina* L. in the Rabigh lagoon, Red Sea. *Saudi J. Biol. Sci.* **2020**, *27*, 1174–1184. [[CrossRef](#)] [[PubMed](#)]
42. Bahrawi, J.A.; Elhag, M.; Aldhebiani, A.Y.; Galal, H.K.; Hegazy, A.K.; Alghailani, E. Soil erosion estimation using remote sensing techniques in Wadi Yalamlam Basin, Saudi Arabia. *Adv. Mater. Sci. Eng.* **2016**, *2016*, 1–8. [[CrossRef](#)]
43. Schmidt, G.L.; Jenkerson, C.B.; Masek, J.; Vermote, E.; Gao, F. Landsat Ecosystem Disturbance Adaptive Processing System (LEDAPS) Algorithm Description. Available online: <https://pubs.er.usgs.gov/publication/ofr20131057> (accessed on 17 March 2015).
44. Vermote, E.; Justice, C.; Claverie, M.; Franch, B. Preliminary analysis of the performance of the Landsat 8/OLI land surface reflectance product. *Remote Sens. Environ.* **2016**, *185*, 46–56. [[CrossRef](#)]
45. Wilson, E.H.; Sader, S.A. Detection of forest harvest type using multiple dates of Landsat TM imagery. *Remote Sens. Environ.* **2002**, *80*, 385–396. [[CrossRef](#)]
46. Qi, J.; Chehbouni, A.; Huete, A.R.; Kerr, Y.H.; Sorooshian, S. A modified soil adjusted vegetation index. *Remote Sens. Environ.* **1994**, *48*, 119–126. [[CrossRef](#)]
47. Fensholt, R.; Horion, S.; Tagesson, T.; Ehammer, A.; Grogan, K.; Tian, F.; Huber, S.; Verbesselt, J.; Prince, S.D.; Tucker, C.J. Assessment of vegetation trends in drylands from time series of earth observation data. In *Remote Sensing Time Series*; Springer: Berlin/Heidelberg, Germany, 2015; pp. 159–182.
48. Ollinger, S.V. Sources of variability in canopy reflectance and the convergent properties of plants. *New Phytol.* **2011**, *189*, 375–394. [[CrossRef](#)]
49. Forkel, M.; Carvalhais, N.; Verbesselt, J.; Mahecha, M.D.; Neigh, C.S.R.; Reichstein, M. Trend change detection in NDVI time series: Effects of inter-annual variability and methodology. *Remote Sens.* **2013**, *5*, 2113–2144. [[CrossRef](#)]
50. Zeileis, A.; Shah, A.; Patnaik, I. Testing, monitoring, and dating structural changes in exchange rate regimes. *Comput. Stat. Data Anal.* **2010**, *54*, 1696–1706. [[CrossRef](#)]
51. Bai, J.; Perron, P. Computation and analysis of multiple structural change models. *J. Appl. Econom.* **2003**, *18*, 1–22. [[CrossRef](#)]
52. Jin, S.; Sader, S.A. Comparison of time series tasseled cap wetness and the normalized difference moisture index in detecting forest disturbances. *Remote Sens. Environ.* **2005**, *94*, 364–372. [[CrossRef](#)]
53. Lugo, A.E.; Snedaker, S.C. The ecology of mangroves. *Annu. Rev. Ecol. Syst.* **1974**, *5*, 39–64. [[CrossRef](#)]
54. Youssef, M.; El-Sorogy, A. Environmental assessment of heavy metal contamination in bottom sediments of Al-Kharrar lagoon, Rabigh, Red Sea, Saudi Arabia. *Arab. J. Geosci.* **2016**, *9*, 474. [[CrossRef](#)]
55. Yahiya, A.B. Environmental degradation and its impact on tourism in Jazan, KSA using remote sensing and GIS. *Int. J. Environ. Sci.* **2012**, *3*, 421–432.

- 
56. Mayr, S.; Kuenzer, C.; Gessner, U.; Klein, I.; Rutzinger, M. Validation of Earth Observation Time-Series: A Review for Large-Area and Temporally Dense Land Surface Products. *Remote Sens.* **2019**, *11*, 2616. [[CrossRef](#)]
  57. Krishnamurthy, P.; Mohanty, B.; Wijaya, E.; Lee, D.-Y.; Lim, T.-M.; Lin, Q.; Xu, J.; Loh, C.-S.; Kumar, P.P. Transcriptomics analysis of salt stress tolerance in the roots of the mangrove *Avicennia officinalis*. *Sci. Rep.* **2017**, *7*, 1–19. [[CrossRef](#)]
  58. Vovides, A.G.; López-Portillo, J.; Bashan, Y. N<sub>2</sub>-fixation along a gradient of long-term disturbance in tropical mangroves bordering the Gulf of Mexico. *Biol. Fertil. Soils* **2011**, *47*, 567–576. [[CrossRef](#)]
  59. Twilley, R.R.; Rivera-Monroy, V.H.; Chen, R.; Botero, L. Adapting an ecological mangrove model to simulate trajectories in restoration ecology. *Mar. Pollut. Bull.* **1999**, *37*, 404–419. [[CrossRef](#)]
  60. Reef, R.; Lovelock, C.E. Regulation of water balance in mangroves. *Ann. Bot.* **2015**, *115*, 385–395. [[CrossRef](#)]